

Electronic Supplementary Information

Facile construction of highly redox active carbons with regular micropores and rod-like morphology towards high-energy supercapacitors

Mulati Mansuer,^a Ling Miao,*^a Dazhang Zhu,^a Hui Duan,^a Yaokang Lv,^c Liangchun Li,^a Mingxian Liu*^{ab} and Lihua Gan*^a

^aShanghai Key Lab of Chemical Assessment and Sustainability, School of Chemical Science and Engineering, Tongji University, Shanghai 200092, P. R. China

^bCollege of Chemistry and Molecular Engineering, Zhengzhou University, Zhengzhou 450001, P. R. China.

^cCollege of Chemical Engineering, Zhejiang University of Technology, Hangzhou 310014, P. R. China

***Corresponding Authors**

E-mail: 1310593@tongji.edu.cn (L. Miao), liumx@tongji.edu.cn (M. Liu), ganlh@tongji.edu.cn (L. Gan)

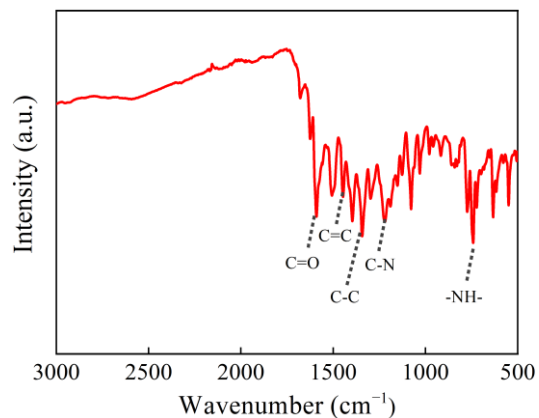


Fig. S1 FT-IR spectrum of the benzoquinone/*p*-phenylenediamine precursor.

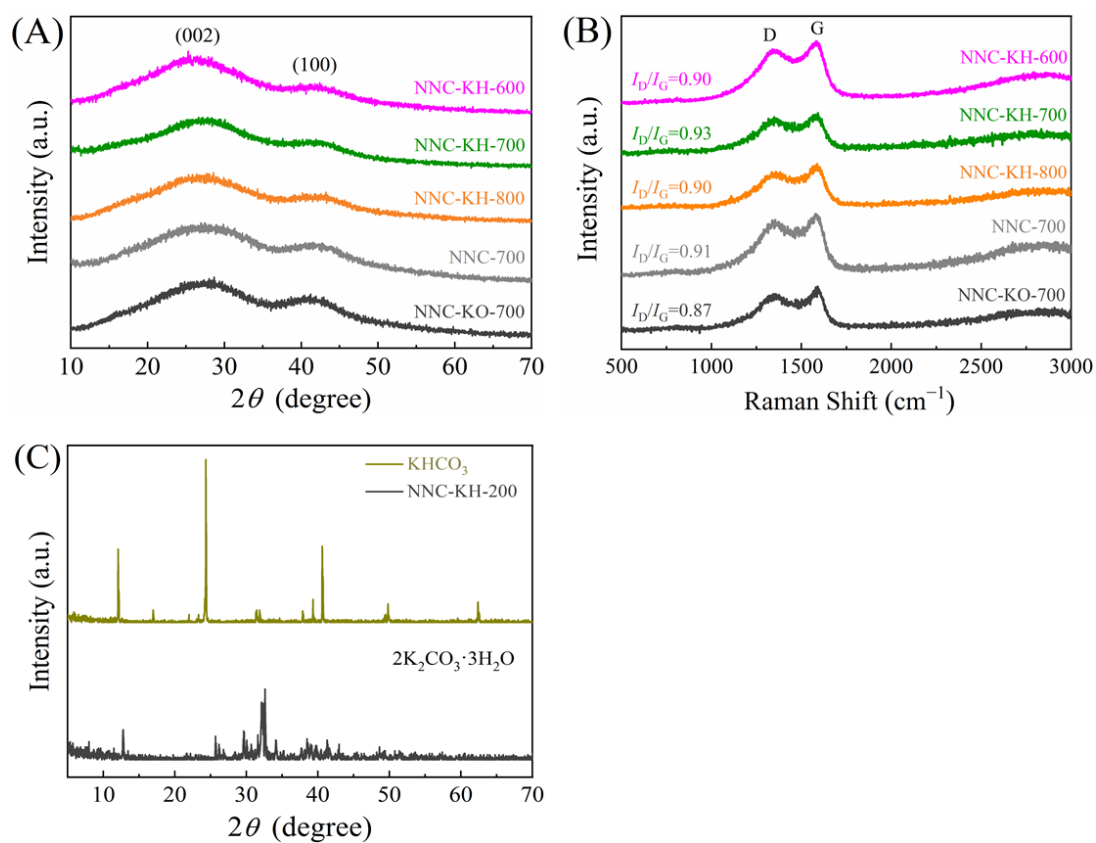


Fig. S2 XRD patterns of NNCs (A). Raman spectra of NNCs (B). XRD patterns of KHCO_3 and NNC-KH-200 (C).

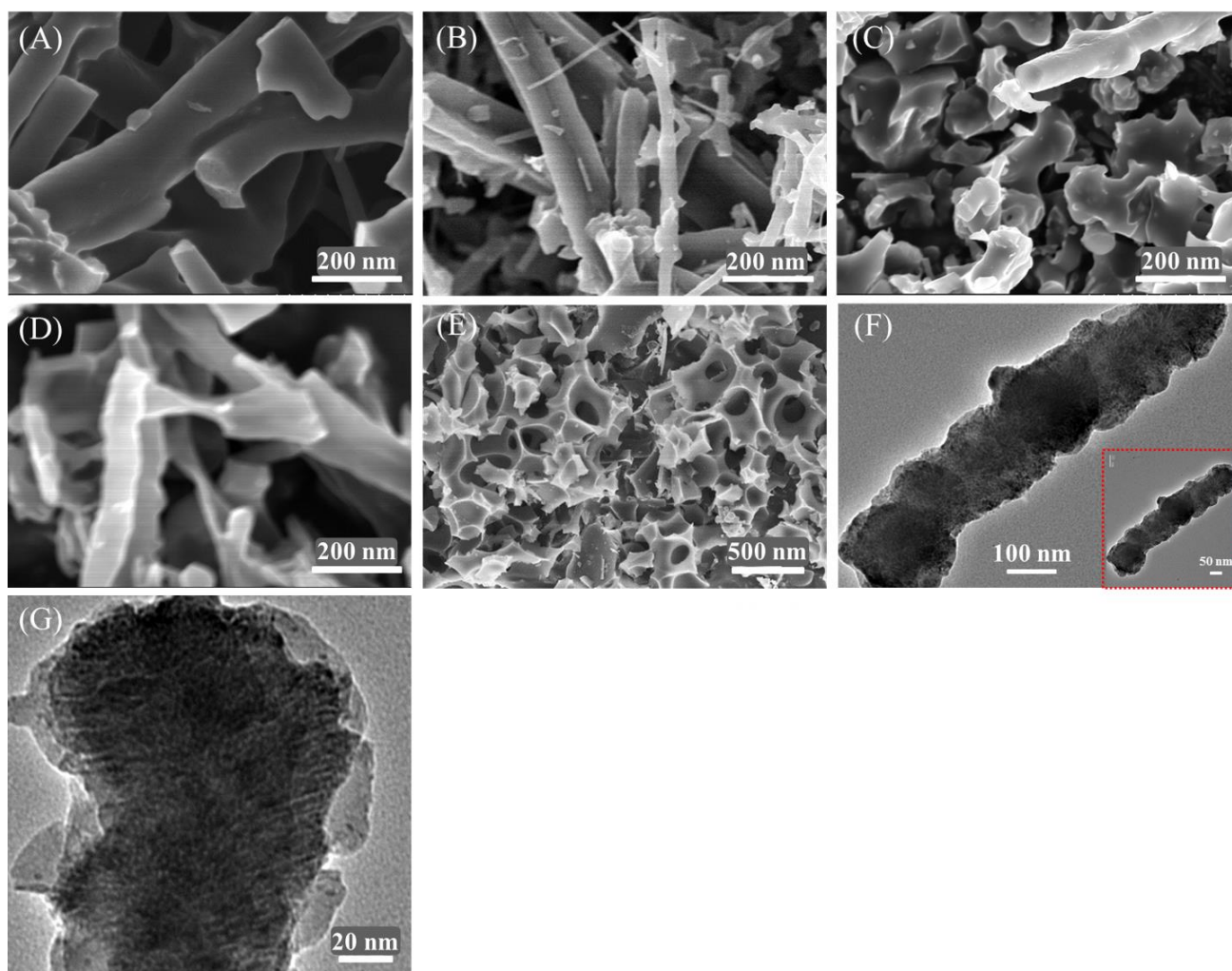


Fig. S3 SEM images of precursor (A), NNC-KH-600 (B), NNC-KH-800 (C), NNC-700 (D), NNC-KO-700 (E). TEM images of typical NNC-KH-700 (F, G).

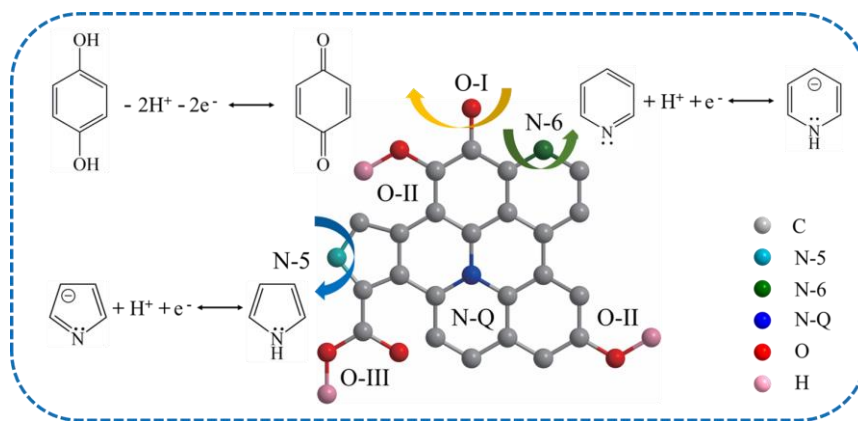


Fig. S4 The locations of faradaic-active species (N-6, N-5 and O-I) in the carbon framework and corresponding redox reactions in acidic solution.

Table S1. The detailed electrochemical data of the devices.^a

Samples	R (Ω)	R_s (Ω)	R_{ct} (Ω)	τ (Ω)	σ ($\Omega \text{ s}^{-0.5}$)	C_E	C_P	C_T	C_P/C_T
						(F g^{-1})	(F g^{-1})	(F g^{-1})	(%)
NNC-KH-600	3.11	1.69	1.42	2.32	0.91	166.9	40.1	207	19.4
NNC-KH-700	1.64	0.56	1.08	0.94	0.74	284.3	80.7	365	22.1
NNC-KH-800	2.64	0.68	1.96	2.95	0.76	231.9	50.1	282	17.8
NNC-700	3.53	1.52	2.01	4.72	0.88	193.7	32.3	226	14.3
NNC-KO-700	3.65	0.76	2.89	2.57	0.80	296.2	39.8	336	11.8

^aAll capacitance values are measured at 1 A g^{-1} .

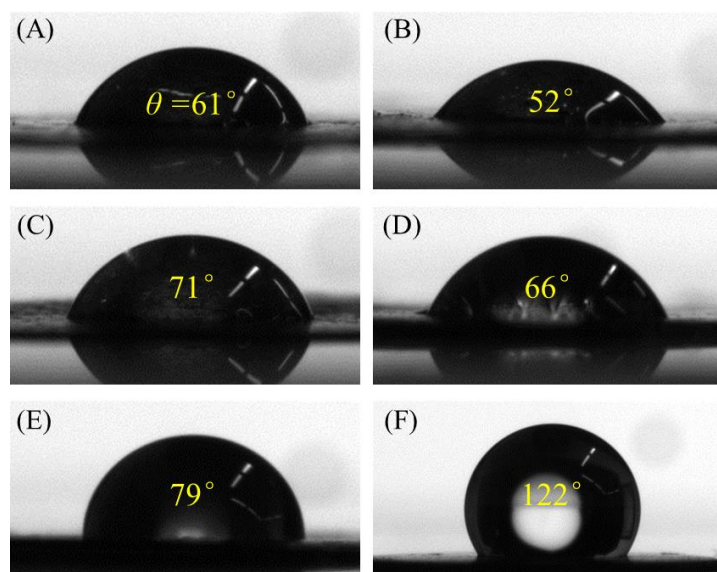


Fig. S5 The water contact angle (θ) measurement results of NNC-KH-600 (A), NNC-KH-700 (B), NNC-KH-800 (C), NNC-700 (D), NNC-KO-700 (E), commercial activate carbon (F).

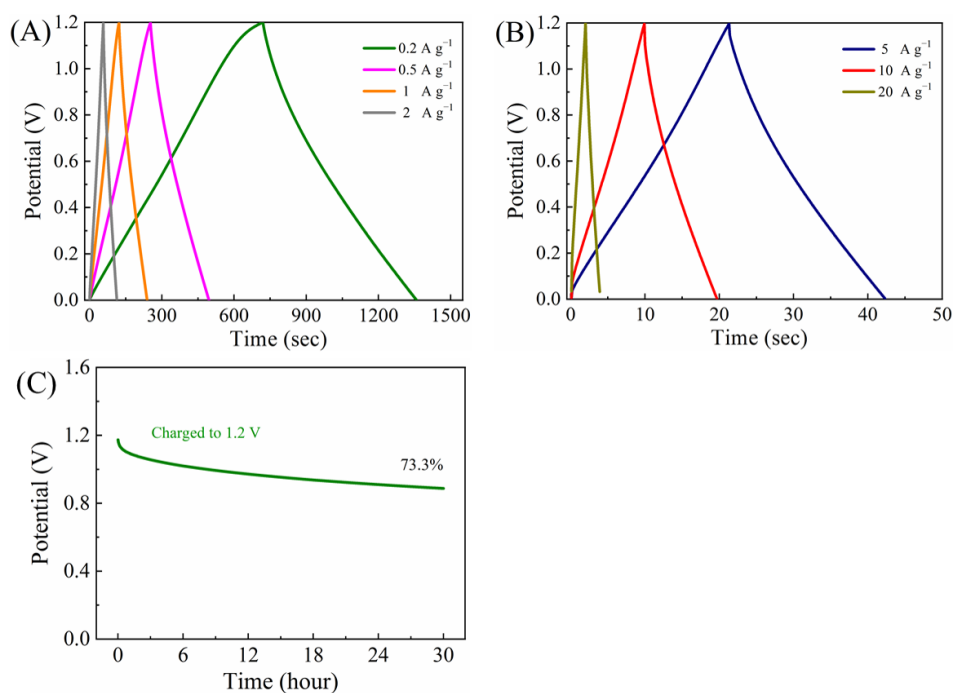


Fig. S6 Electrochemical performances of the symmetric coin-typed cell based on NNC-KH-700 electrode using $\text{H}_2\text{SO}_4+\text{KBr}$ electrolyte: GCD curves of NNC-KH-700 at different current densities from 0.2 to 20 A g^{-1} (A, B). Self-discharge curve within the potential window of 0–1.2 V (C).

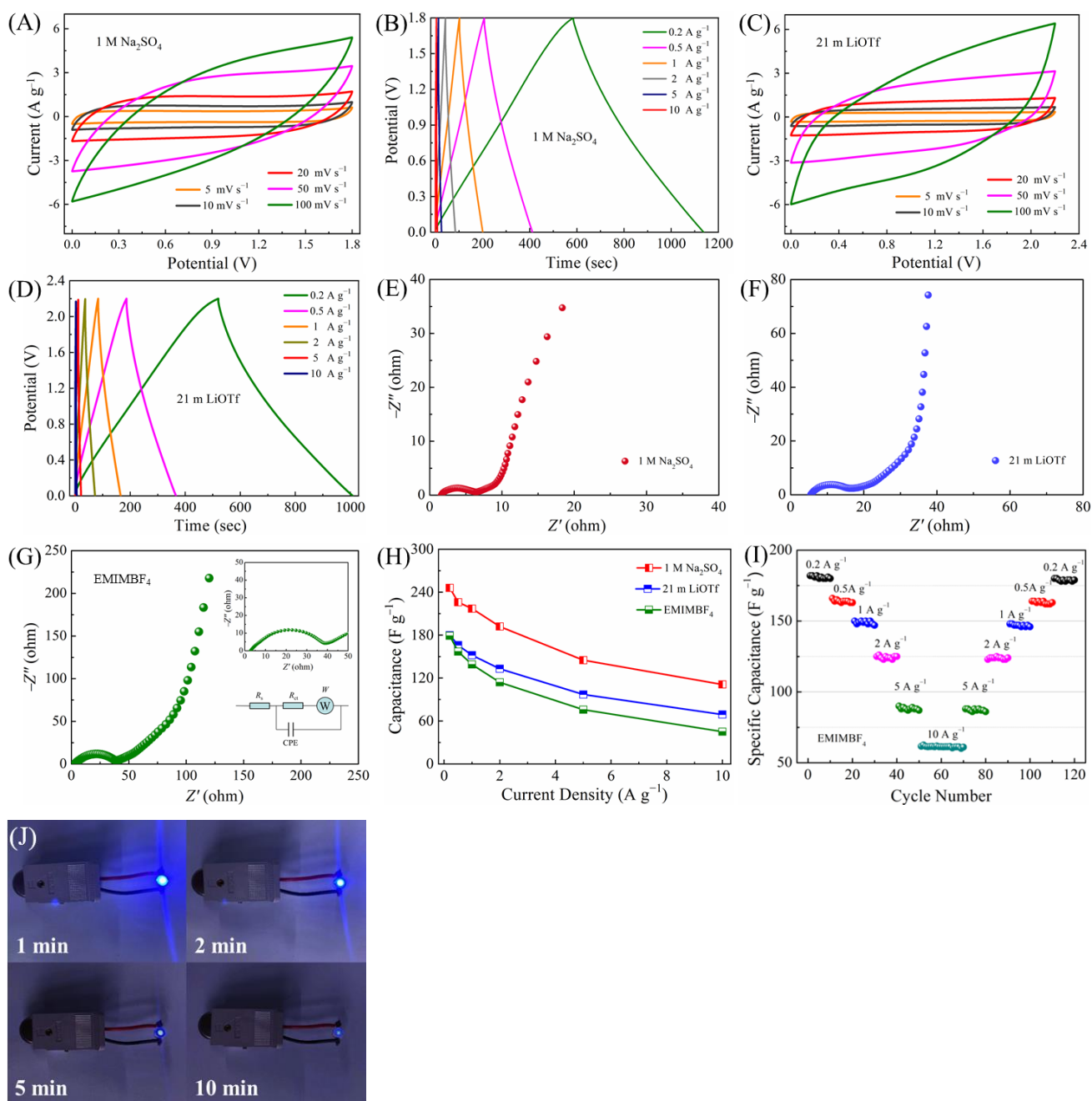


Fig. S7 Electrochemical performances of the symmetric coin-typed cell based on NNC-KH-700 electrode: CV curves at different scan rates for 1 M Na₂SO₄ (A). GCD curves at various current densities for 1 M Na₂SO₄ (B). CV curves at different scan rates for 21 m LiOTf (C). GCD curves at various current densities for 21 m LiOTf (D). Nyquist plots for 1 M Na₂SO₄ (E) and for 21 m LiOTf (F). Nyquist plot and equivalent series resistance for EMIMBF₄ (G). Capacitances vs current densities (H). Rate performance (I). Images of powered up LED using EMIMBF₄ electrolyte (J).

Table S2. Performance comparisons of reported carbon-based devices.

Samples	N/O Content (wt.%)	Specific Surface Area (m ² g ⁻¹)	Electrolyte	Specific Capacitance (F g ⁻¹)	Energy Density (W h kg ⁻¹)	References
NNC-KH-700	11.46/10.11	1840	H ₂ SO ₄ +KBr	365	18.25	This work
			1 M Na ₂ SO ₄	248	24.4	
			21 m LiOTf	180	30.1	
			EMIMBF ₄	179	89.5	
TCNQ-CTF-800	8.13/-	3663	EMIMBF ₄	100	42.8	1
Ta-NCa ₈₅₀	7.26/8.24	706	1 M H ₂ SO ₄	362	-	2
NO-PC	2.2/4.8 at.%	3794	6 M KOH	269	18.9	3
a-CNS/EG-10	5.3/-	1532	PVA/KOH	234	6.3	4
HMC-800	4.74/5.53	1306	1 M LiPF ₆	126	29	5
N1-GDY	3.7/2.65	-	7 M KOH	250	8.66	6
C-silkworm	2.15/12.58 at.%	2258	1 M Na ₂ SO ₄	167	23.17	7
CNS-800	4.9/-	1122	KOH/PVA	190	-	8
N/S-HPCM	5.13/- at.%	927	1 M Na ₂ SO ₄	127	17.6	9
CBC3	6.2/10.4 at.%	3534	6 M KOH	297	18	10

References

1. Y. Li, S. Zheng, X. Liu, P. Li, L. Sun, R. Yang, S. Wang, Z. S. Wu, X. Bao and W. Q. Deng, Conductive microporous covalent triazine-based framework for high-performance electrochemical capacitive energy storage, *Angew. Chem. Int. Ed.*, 2018, **57**, 7992–7996.
2. Y. Li, L. Liu, Y. Wu, T. Wu, H. Wu, Q. Cai, Y. Xu, B. Zeng, C. Yuan and L. Dai, Facile synthesis of nitrogen-doped carbon materials with hierarchical porous structures for high-performance supercapacitors in both acidic and alkaline electrolytes, *J. Mater. Chem. A*, 2019, **7**, 13154–13163.
3. Y. Zhao, M. Wei, Z. Zhu, J. Zhang, L. Xiao and L. Hou, Facile preparation of N-O codoped hierarchically porous carbon from alginate particles for high performance supercapacitor, *J. Colloid Interface Sci.*, 2020, **563**, 414–425.
4. Y. Liu, X. Qiu, X. Liu, Y. Liu and L.-Z. Fan, 3D porous binary-heteroatom doped carbon nanosheet/electrochemically exfoliated graphene hybrids for high performance flexible solid-state supercapacitors, *J. Mater. Chem. A.*, 2018, **6**, 8750–8756.
5. W. Qian, F. Sun, Y. Xu, L. Qiu, C. Liu, S. Wang and F. Yan, Human hair-derived carbon flakes for electrochemical supercapacitors, *Energy Environ. Sci.*, 2014, **7**, 379–386.
6. H. Shang, Z. Zuo, H. Zheng, K. Li, Z. Tu, Y. Yi, H. Liu, Y. Li and Y. Li, N-doped graphdiyne for high-performance electrochemical electrodes, *Nano Energy*, 2018, **44**, 144–154.
7. S. Lei, L. Chen, W. Zhou, P. Deng, Y. Liu, L. Fei, W. Lu, Y. Xiao and B. Cheng, Tetra-heteroatom self-doped carbon nanosheets derived from silkworm excrement for high-performance supercapacitors, *J. Power Sources*, 2018, **379**, 74–83.
8. T. Wei, X. Wei, L. Yang, H. Xiao, Y. Gao and H. Li, A one-step moderate-explosion assisted carbonization strategy to sulfur and nitrogen dual-doped porous carbon nanosheets derived from

camellia petals for energy storage, *J. Power Sources*, 2016, **331**, 373–381.

9. L. Sun, Y. Zhou, L. Li, H. Zhou, X. Liu, Q. Zhang, B. Gao, Z. Meng, D. Zhou and Y. Ma, Facile and green synthesis of 3D honeycomb-like N/S-codoped hierarchically porous carbon materials from bio-protic salt for flexible, temperature-resistant supercapacitors, *Appl. Surf. Sci.*, 2019, **467–468**, 382–390.
10. D. Qiu, M. Li, C. Kang, J. Wei, F. Wang and R. Yang, Cucurbit[6]uril-derived sub-4 nm pores-dominated hierarchical porous carbon for supercapacitors: operating voltage expansion and pore size matching, *Small*, 2020, **16**, 2002718.